

SIMULATION STUDY OF ELECTRON BEAM ACCELERATION WITH NON-GAUSSIAN TRANSVERSE PROFILES FOR AWAKE RUN 2

L. Liang^{*1}, G. Xia¹, University of Manchester, Manchester, United Kingdom
J. P. Farmer², Max Planck Institute for Physics, Munich, Germany
¹also at Cockcroft Institute, Daresbury, United Kingdom
²also at CERN, Geneva, Switzerland

Abstract

In the physics plan for AWAKE Run 2, two known effects, beam loading the longitudinal wakefield and beam matching to the pure plasma ion channel, will be implemented for the better control of electron acceleration. It is founded in our study of beam matching that the transverse profile of the initial witness beam have a significant impact on its acceleration quality. In this paper, particle-in-cell (PIC) simulations are used to study factors that affect the acceleration quality of electron beams with different transverse profiles.

INTRODUCTION

The Advanced Wakefield Experiment (AWAKE) at CERN has successfully achieved the acceleration of externally-injected electrons to 2 GeV in the proton-driven wakefield for the first time [1]. Inspired by the success of Run 1 experiment, AWAKE Run 2 aims to accelerate an electron bunch to higher energy while maintaining a relatively narrow energy spread and a controllable emittance growth [2]. To meet these goals, two known effects, beam loading and beam matching, are anticipated to be used in AWAKE Run 2 [3,4]. The concept of beam loading is to minimize the witness beam's energy spread by finely tuning the delay between the driver and witness bunch to flatten the accelerating field. And the idea of beam matching is to match the beam's emittance to the plasma focusing force to prevent the envelope oscillation. The matched beam radius can be expressed as

$$\sigma_{rm} = \sqrt[4]{\frac{2\epsilon_n^2}{\gamma_{eb}k_p^2}}, \quad (1)$$

where $k_p = \omega_p/c$ is the plasma wave number, ϵ_n is the normalized emittance of the electron bunch, and γ_{eb} is the relativistic gamma factor of the e-beam. In $k_p = \omega_p/c$, c is the speed of light, and $\omega_p = \sqrt{n_0 e^2 / m \epsilon_0}$ is the plasma frequency, where m is the electron mass, ϵ_0 is the vacuum permittivity, n_0 is the plasma density, and e is the elementary charge.

Previous study [4] of the matching condition as well as beam loading is based on the assumption that the beam has a bi-Gaussian transverse spatial profile, which may not be the exact case when beam bunches are transported along the beamline to the injection point. The beam can naturally develop a rectangular-like distribution by folding on top of

itself in phase space, or a Christmas-tree-like distribution due to the betatron mismatch and filamentation [5].

For 1D beam spatial distributions with a Gaussian-like profile, they are equivalent if they have the same first and second moments, i.e., the same centroid displacement $\langle x \rangle$ and r.m.s. beam radius $\sigma_x = \sqrt{\langle x^2 \rangle}$. In order to characterize the tailedness or the peakedness of a 1D spatial distribution to quantify its deviation from the normal distribution, several statistical descriptions have been proposed for this purpose [6]. One widely adopted parameter is *kurtosis*, the normalized fourth moment of the distribution (see Eq. (3) in Appendix). The kurtosis is already a good indicator of the visually observable halo. However, simulations show that halo can "hide" in the phase space and is not observed in some spatial projections. So a more representative parameter, the *halo parameter* (see Eq. (4) in Appendix), is introduced to quantify beam's halo factor after acceleration in this proceeding. The *halo parameter* is basically the 2D form kurtosis in the phase space. And it is an invariant under the linear transverse focusing force in the pure ion channel, which can be formed in the blow-out regime [7].

The aim of this study is to investigate the impact of the non-Gaussian beam spatial distributions, e.g. the super Gaussian distribution, on the beam's acceleration quality, such as emittance, envelope evolution, etc., which could affect the performance of the future plasma wakefield acceleration (PWFA) based applications [8].

SIMULATION PARAMETERS

The simulation of this work uses the toy model that was first introduced in the study of beam loading in [4]. This model makes use of a single, short, non-evolving proton bunch as the driver to mimic the quasi-linear wakefield driven by the self-modulated SPS proton bunch. A high-density witness electron bunch is injected on axis and close to the crest of the accelerating field. The high-density witness itself will drive a plasma-electron-free 'bubble' behind its head. The 'bubble' will provide uniform self-focusing force for the rear part of the witness. The loading position (time delay w.r.t the proton driver) and witness parameters are carefully chosen to form a region with uniform accelerating field so as to reduce the energy spread, as shown in Fig. 1.

Simulations in this work are carried out with the 3D quasi-static particle-in-cell (PIC) code QV3D [9], built on the VLPL platform [10]. In all considered cases, the witness electron bunch has a Gaussian profile in the longitudinal

* linbo.liang@postgrad.manchester.ac.uk

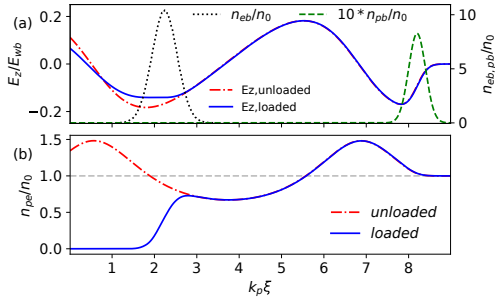


Figure 1: QV3D simulation results showing the plasma wakefields (a) and plasma electron density (b) on the propagation axis at the beginning ($t = 0$). The unloaded case (dash-dotted line), without witness (grey dotted line), and the loaded case (solid line), with both the proton driver (green dashed line) and electron witness, are shown for comparison. Solid line with ‘x’ marker is the transverse wakefield.

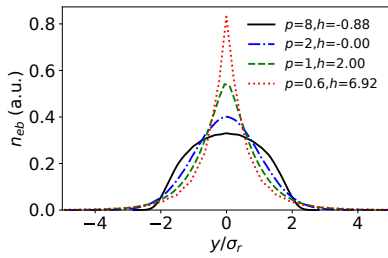


Figure 2: The 1D density distribution for the super Gaussian transverse beam profile with identical r.m.s. beam size.

direction, with the r.m.s bunch length $\sigma_{ze} = 60 \mu\text{m}$, and a radial super Gaussian distribution with form parameter p in the transverse planes. The super Gaussian function can be expressed as follows [5]:

$$n(y) \propto e^{-|y|^p}. \quad (2)$$

Shown in Fig. 2 is the 1D density distribution following Eq. (2), where $p = 2$ corresponds to the form of a normal distribution, $p < 2$ refers to those heavy tailed bunch profile, and $p > 2$ is the light tailed case. The transverse r.m.s size σ_{re} is normalized to the matched beam radius σ_{rm} . For a uniform plasma density of $n_0 = 7 \times 10^{14} \text{ cm}^{-3}$, which corresponds to the AWAKE Run 2 high density case [3], and an electron bunch with initial energy of 150 MeV ($\gamma_{eb} = 294.54$) and normalized emittance of $\epsilon_n = 7 \mu\text{m}$, Eq. (1) yields the matched beam radius $\sigma_{rm} = 10.764 \mu\text{m}$. The relative energy spread is 0.1%. The electron bunch charge is chosen as 120 pC, corresponding to a normalized peak density $n_{eb}/n_0 = 9.77$. The proton driver’s energy is 400 GeV ($\gamma_{pb} = 426.29$), and other parameters are the same as that in [4].

The simulations are conducted by employing a speed-of-light moving window with the sizes $(9 \times 6 \times 6)k_p^{-1}$ and resolution $(0.01 \times 0.01 \times 0.01)k_p^{-1}$ in directions of (x, y, z) , where x is the longitudinal direction, y and z are transverse

directions. The time step is chosen as small as $10\omega_p^{-1}$ to resolve the witness particles’ betatron motion. The number of particles per cell is 4 for plasma with fixed ion background and 1 for the non-evolving proton driver. The witness beam is simulated with 10^6 equally-weighted macro particles.

RESULTS AND DISCUSSION

Figure 3 (a) shows the normalized emittance of the witness beam, taken as $\epsilon_n = \sqrt{\epsilon_{ny} * \epsilon_{nz}}$ for cases with different initial kurtosis h_0 , where ϵ_{ny} and ϵ_{nz} are the directional components in two transverse planes. The corresponding slice emittance along the accelerated beam is also shown in subplot (b). One can see that for all considered cases, the projected emittance only increases in the first tens of centimetres, then remains almost constant during the following acceleration. But the final values are different w.r.t the initial kurtosis h_0 . Beam distributions with a non-zero kurtosis ($h_0 \neq 0$) have relatively lower stabilized projected emittance than the Gaussian case with $h_0 = 0$. Fig. 3 (b) further indicates that the emittance growth mainly occurs at the head of beam, which is mostly outside the ‘bubble’ and not benefit from the strong uniform focusing force (See Fig. 1). The beam head experiences intensive betatron oscillations at the first half meter. However, under the non-linear focusing force of the proton driven wakefield, the emittance of the head part also stabilizes after the betatron oscillations being damped due to phase-mixing. For all considered cases, the rear part of the electron beam within the bubble generally retains its initial emittance during the acceleration.

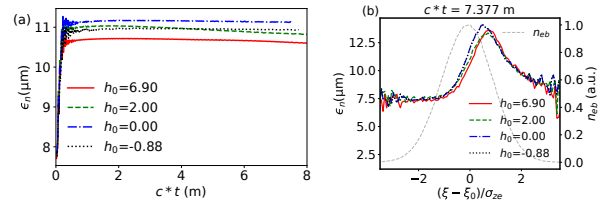


Figure 3: The witness beam’s normalized projected emittance (a) and the corresponding slice emittance (b) along the beam that sampled at $c * t = 7.377$ m.

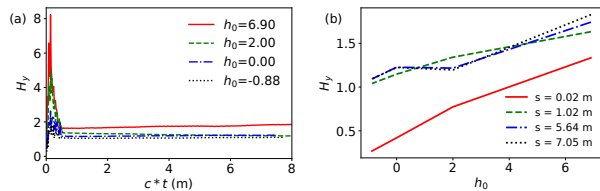


Figure 4: The halo parameter H in y -plane.

Figure 4 (a) shows the evolution of beam’s halo parameter. For all the cases, the halo parameter increases significantly in the first half metre, similar to the behaviour of the projected emittance, and then falls back to a stable value that is higher than the initial one. The maximum H that can be reached and

the final value is positively correlated with initial kurtosis, as shown in Fig. 4 (b).

Figure 5 shows the witness beam's brightness $B = I_{eb}/\epsilon_{ny}\epsilon_{nz}$, where I_{eb} is the beam current. The brightness measures the achievable current density for a given beam divergence. Although there is no significant difference of brightness for considered cases, one can still see that the beam with a high initial kurtosis has a higher brightness.

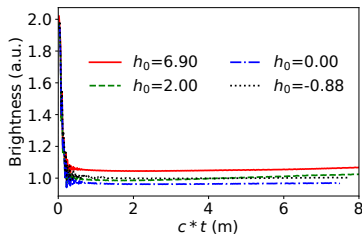


Figure 5: The witness beam's brightness w.r.t. propagation distance.

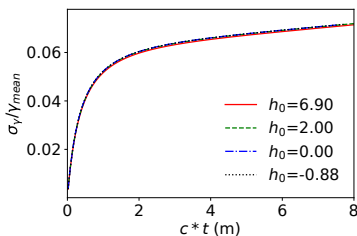


Figure 6: Relative energy spread of the witness beam w.r.t. propagation distance.

Figure 6 shows the relative energy spread of the witness beam. As aforementioned, the energy spread of the witness beam is mainly caused by the non-uniformity of longitudinal wakefields along the beam, so the relative energy spread of the full beam is almost identical for all cases.

CONCLUSION

In this study, we found that the initial *kurtosis* of a non-Gaussian transverse beam profile can have significant impact on the beam quality during acceleration. It is shown that beam metrics being investigated in this proceeding will stay on or approach a nearly stabilized value soon after ~ 1 m propagation. But the final values of beam's halo parameter and the brightness have a positive correlation with transverse profile's initial kurtosis. A beam profile with matched radius and large initial kurtosis will show higher brightness after acceleration, which may have positive impact for applications of future PWFA-based high energy physics.

ACKNOWLEDGMENTS

The authors would like to acknowledge the support from the Cockcroft Institute Core Grant and the STFC AWAKE

Run 2 grant ST/T001917/1. Computing resources are provided by the SCARF HPC of STFC and the CERN HPC services.

APPENDIX

Kurtosis Kurtosis, denoted by h , is defined as the standardized fourth moment, given as [6]:

$$h = \langle x^4 \rangle / \langle x^2 \rangle^2 - 3, \quad (3)$$

where $\langle x^n \rangle = \frac{1}{N} \sum_{i=1}^N (x_i - \bar{x})^n$ is the n -th moment about the mean, and \bar{x} is the mean. The above expression of kurtosis will naturally make its value normalized to that of the standard Gaussian distribution, i.e., $h = 0$.

Halo parameter The *halo parameter* is given as [6]:

$$\begin{aligned} H &= \sqrt{3I_4} / (2I_2) - 3, \\ I_2 &= \langle x^2 \rangle \langle x'^2 \rangle - \langle xx' \rangle^2, \\ I_4 &= \langle x^4 \rangle \langle x'^4 \rangle + 3 \langle x^2 x'^2 \rangle^2 - 4 \langle xx'^3 \rangle \langle x^3 x' \rangle, \end{aligned} \quad (4)$$

where $x' = dx/dz \approx p_x/p_z$ and $\langle x^m x'^n \rangle = \frac{1}{N} \sum_{i=1}^N (x_i - \bar{x})^m (x'_i - \bar{x}')^n$. The I_2 factor is exactly the square of beam's geometric emittance. The constant is chosen to be consistent with the definition of kurtosis.

REFERENCES

- [1] M. Turner *et al.*, "Experimental Observation of Plasma Wakefield Growth Driven by the Seeded Self-Modulation of a Proton Bunch", *Phys. Rev. Lett.*, vol. 122, no. 5, p. 054801, 2019. doi:10.1103/PhysRevLett.122.054801
- [2] E. Gschwendtner, "Awake Run 2 at CERN", presented at the 12th Int. Particle Accelerator Conf. (IPAC'21), Campinas, Brazil, May 2021, paper TUPAB159.
- [3] P. Muggli, "Physics to plan AWAKE Run 2", *J. Phys. Conf. Ser.*, vol. 1596, p. 012008, 2020. doi:10.1088/1742-6596/1596/1/012008
- [4] V. K. B. Olsen, E. Adli, and P. Muggli, "Emittance preservation of an electron beam in a loaded quasilinear plasma wakefield", *Phys. Rev. Accel. Beams*, vol. 21, no. 1, p. 011301, 2018. doi:10.1103/PhysRevAccelBeams.21.011301
- [5] F. J. Decker, "Beam distributions beyond RMS", *AIP Conf. Proc.*, vol. 333, no. 1, pp. 550-556, 1995. doi:10.1063/1.48035
- [6] C. K. Allen and T. P. Wangler, "Parameters for Quantifying Beam Halo", in *Proc. 19th Particle Accelerator Conf. (PAC'01)*, Chicago, IL, USA, Jun. 2001, paper TPPH032, pp. 1732-1734.
- [7] W. Lu, C. Huang, M. Zhou, W. B. Mori, and T. Katsouleas, "Nonlinear theory for relativistic plasma wakefields in the blowout regime", *Phys. Rev. Lett.*, vol. 96, no. 16, p. 165002, Apr. 2006. doi:10.1103/PhysRevLett.96.165002
- [8] S. Papadopoulou *et al.*, "Impact of non-Gaussian beam profiles in the performance of hadron colliders", *Phys. Rev. Accel. Beams*, vol. 23, no. 10, p. 101004, 2020. doi:10.1103/PhysRevAccelBeams.23.101004

- [9] A. Pukhov, "Particle-In-Cell Codes for Plasma-based Particle Acceleration", CERN, Geneva, Switzerland, Rep. CERN-2016-001.181, Oct. 2015.
- [10] A. Pukhov, "Three-dimensional electromagnetic relativistic particle-in-cell code VLPL (Virtual Laser Plasma Lab)", *J. Plasma Phys.*, vol. 61, no. 3, pp. 425-433, 1999.
doi:10.1017/S0022377899007515